CrossMark

Mechanisms of inorganic carbon-14 attenuation in contaminated groundwater: Effect of solution pH on isotopic exchange and carbonate precipitation reactions

Aislinn A. Boylan [a], Douglas I. Stewart [b], James T. Graham [c], Divyesh Trivedi [d], Ian T. Burke [a, *]

[a] School of Earth and Environment, University of Leeds, Leeds, LS2 9JT, UK
[b] School of Civil Engineering, University of Leeds, Leeds, LS2 9JT, UK
[c] National Nuclear Laboratory, Sellafield, Cumbria, CA20 1PG, UK
[d] National Nuclear Laboratory, Risley, Warrington, Cheshire WA3 6AE, UK

ARTICLE INFO

ABSTRACT

Radioactive ^{14}C is a significant contaminant associated with nuclear fuels and wastes that is potentially highly mobile in the environment as dissolved inorganic carbonate species. This study investigated the mechanisms by which dissolved inorganic ^{14}C is retained in surface and groundwater environments via precipitation and isotopic exchange reactions. Precipitation of calcite in the presence and absence of nucleation sites is considered along with isotopic exchange with both atmospheric CO_2 and solid carbonates. Precipitation occurs at calcite supersaturation values of $SI_{CAL} > 1.5$ in the absence of nucleation sites and $SI_{CAL} > 0{-}0.5$ in the presence of nucleation sites, suggesting that precipitation of ^{14}C-bearing carbonates is much more likely in subsurface environments where nucleation sites are abundant. The maximum ^{14}C removal in solid isotopic exchange experiments occurred after approximately 2 weeks equilibration. In these experiments the amount of ^{14}C removed from solution was proportional to the amount of calcite surface area present, and removal from solution was equivalent to rapid equalisation of the isotope ratio in an 8–10 Å active surface layer. Although the reactivity of natural carbonates may be lower than the calcite samples used in this study, these results suggest isotopic exchange with solids will be an important ^{14}C retardation mechanism in subsurface environments containing only modest TIC concentrations. These results suggest that if inorganic ^{14}C is released into sub-surface environments, both precipitation and solid phase isotopic exchange can result in non-conservative ^{14}C-DIC transport and ^{14}C contamination may persist in groundwater for decades following accidental releases. In contrast, in experiments open to atmosphere with pH values below 9.3, complete loss of dissolved inorganic ^{14}C was very rapid and occurred with timescales of 10's of hours. ^{14}C loss was due to a rapid exchange of dissolved ^{14}C species with $^{12}CO_2$ (g) and the kinetics of ^{14}C removal increased as pH values were lowered (i.e. atmospheric isotopic exchange was first order with respect to the concentration of carbonic acid present). Thus these results suggest that release of inorganic ^{14}C to surface waters with pH values <9.3 would result in rapid exchange with $^{12}CO_2$ (g) and ^{14}C would not persist in the aqueous environment, whereas ^{14}C-DIC released to saturated subsurface environments may persist close to the release site for decades due to precipitation and solid phase exchange reactions preventing/retarding transport with the groundwater.

1. Introduction

The carbon isotope, ^{14}C, is a widespread β-emitting radionuclide that is produced both naturally and anthropogenically. It is produced due to stratospheric irradiation of ^{14}N as well as at each stage of the nuclear fuel cycle from the parent isotopes ^{14}N, ^{17}O and ^{13}C

* Corresponding author.
  E-mail address: I.T.Burke@leeds.ac.uk (I.T. Burke).

(Eabry et al., 1995; Yim and Caron, 2006). Natural and anthropogenic ^{14}C production are of similar magnitude, however natural production is globally dispersed while anthropogenic sources are highly localised within nuclear sites (Magnusson et al., 2004; Roussel-Debet et al., 2006). At nuclear sites, ^{14}C is an important radioactive contaminant because of its long half-life (5730 ± 40a) (Godwin, 1962) and its ability to bioaccumulate in plants and animals (Begg et al., 1992; Cook et al., 1998; Yim and Caron, 2006). Most ^{14}C formed in nuclear reactors is generated as inorganic species (e.g. carbide and ^{14}CO$_2$) during energy production leading to a large ^{14}C solid waste inventory for disposal (Yim and Caron, 2006; Boss and Allsop, 1995). As ^{14}C is a potentially very mobile component of radioactive wastes, many studies have focussed on the expected ^{14}C behaviour after disposal in deep geological facilities (Yim and Caron, 2006; Bracke and Müller, 2008; Marshall et al., 2011; Baston et al., 2012; NDA, 2012; Doulgeris et al., 2015). Due to the strongly reducing conditions anticipated in repositories, and because aqueous inorganic ^{14}C (^{14}C-DIC) tends to rapidly precipitate as solid carbonates within alkaline cementitious backfills, most studies have concentrated on the production and transport of radiolabelled methane (^{14}CH$_4$), (e.g. Jackson and Yates, 2011; Limer et al., 2011, 2013; Marshall et al., 2011). Less research has been undertaken on the environmental mobility of inorganic ^{14}C in shallow subsurface environments, despite the risk of its accidental release to such environments during waste reprocessing and storage.

Due to its ubiquity in the nuclear power generation process ^{14}C-containing wastes are generated and released at every power station and reprocessing site worldwide, both as regulated discharges to air and water, as well as accidental releases at some sites (Yim and Caron, 2006). ^{14}C contamination was first identified due to discharge from the low level waste trenches storing ^{14}C inventory at Chalk River Site, Canada. Historical leaks from this storage area of the facility have led to ^{14}C plumes reaching the natural environment, particularly a nearby wetland. This has led to a series of studies into the behaviour of ^{14}C in natural environments (Evenden et al., 1998; Killey et al., 1998; Bird et al., 1999). In the UK the most significant example of ^{14}C contamination is associated with the nuclear fuel reprocessing plant at Sellafield, Cumbria (Stamper et al., 2012; Marshall et al., 2015) with the major source being water leaks from the intermediate level waste storage facilities in the 1970's (Marshall et al., 2015). Specifically ^{14}C-containing liquor was lost from silos holding corroded magnesium alloy (MAGNOX) fuel cladding. The liquor had a pH of 9–11 due to equilibration with the fuel cladding (Wallace et al., 2012; Parry et al., 2011) and ^{14}C is thought to have been present predominately as the inorganic species H^{14}CO$_3^-$ and ^{14}CO$_3^{2-}$.

In soil, inorganic carbon can exist as gaseous carbon dioxide, aqueous species, sorbed species and solid carbonates. Transitions between these phases are controlled by pH, pCO$_2$, the cations in solution, and the presence of interfaces (e.g. Langmuir, 1997; Inskeep and Bloom, 1985; van Geen et al., 1994; Hodkin et al., 2016). In systems open to atmosphere aqueous CO$_2$ concentrations reach equilibrium with atmospheric pCO$_2$ (Atkins and De Paula, 2006). Dissolved inorganic carbon (DIC) is distributed between CO$_2$(aq), carbonic acid (H$_2$CO$_3$(aq)), the bicarbonate anion (HCO$_3^-$) and carbonate anion (CO$_3^{2-}$) depending on the solution pH (see equations 1–4 below) (Greenwood and Earnshaw, 1997; Langmuir, 1997). Dissociation constants (pK$_a$) of carbonic acid – bicarbonate – carbonate are 3.6 and 10.3 respectively (at 25 °C and zero ionic strength; Plummer and Busenberg, 1982). In open systems at high pH, therefore, the continuing equilibrium between atmospheric and dissolved CO$_2$ (i.e. CO$_2$ in gassing) can result in very high DIC values (Stumm and Morgan, 1996).

Carbonate species do not sorb to quartz sand or montmorillonite

$CO_{2(g)} \rightleftharpoons CO_{2(aq)}$	Fast	(Equation 1)
$H_2O + CO_{2(aq)} \rightleftharpoons H_2CO_{3(aq)}$	Slow	(Equation 2)
$H_2CO_{3(aq)} \rightleftharpoons HCO_{3(aq)}^- + H_{(aq)}^+$	Fast	(Equation 3)
$HCO_{3(aq)}^- \rightleftharpoons CO_{3(aq)}^{2-} + H_{(aq)}^+$	Fast	(Equation 4)

(adapted from Greenwood and Earnshaw, 1997).

at circumneutral pH (Garnier, 1985; Sheppard et al., 1998), suggesting that carbonate species interact poorly with both silica and the silicate layer of clays. However ^{14}C-DIC species can adsorb to soil minerals such as aluminium and iron oxides at circumneutral pH values (Su and Suarez, 1997). For example HCO$_3^-$ was found to adsorb to goethite surfaces at ~pH7 as an inner-sphere carbonate surface complex by a ligand exchange reaction probably with singly coordinated Fe-OH and Al-OH surface groups (Wijnja and Schulthess, 2000; Su and Suarez, 1997). However sediment composition is usually dominated by silicate minerals, so anion exchange is a less effective process than cation exchange (negatively charged surface sites are present at much high densities than positive surface sites; Gu and Schulz, 1991). Therefore in many environments the aqueous transport of DIC is relatively unretarded (i.e. in the absence of precipitation reactions, it will move at approximately the same rate as groundwater flow).

In typical groundwater systems, precipitation of carbonate minerals is controlled by pH and the concentration of divalent cations. The relative propensity for carbonate to precipitate from solution is governed principally by the ratio of the ion activity products (IAP $= a$Me$^{2+}_{(aq)} \cdot a$CO$_3^{2-}_{(aq)}$) to the mineral solubility product at equilibrium (the saturation index, SI $= \log_{10}$(IAP/K$_{sp}$)) for reactions with the form:

$$Me^{2+}_{(aq)} + CO_3^{2-}(aq) \rightleftharpoons MeCO_{3(s)} \qquad (5)$$
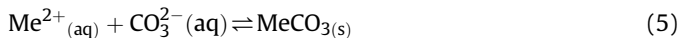
where Me$^{2+}_{(aq)}$ is a divalent metal ion, and a is the activity of the aqueous ion (when SI > 0 precipitation is thermodynamically favoured, and when SI < 0 dissolution is thermodynamically favoured).

In relatively oxic near surface groundwater environments calcium is usually the most abundant divalent cation. Magnesium can also be relatively abundant however, other divalent species (e.g. Sr^{2+}; Ba^{2+}; Fe^{2+} etc.) are normally only present as trace components (Krauskopf and Bird, 1995). Although a wide range of different solid carbonate phases are possible (e.g. calcite, aragonite, magnesite and dolomite), at low temperature and pressures, calcite (CaCO$_3$) is the predominant carbonate phase expected. It is often magnesium substituted (Ca(Mg)CO$_3$) where aqueous Mg^{2+} is present during crystallisation (Mucci and Morse, 1983; Bischoff et al., 1983). In the absence of nucleation sites, calcite will precipitate homogeneously from a supersaturated calcium carbonate solution when the saturation index, SI > ~1.5, and it will occur heterogeneously when SI > ~0.3 where solid substrate provides nucleation sites (Ford and Williams, 2007). In the subsurface environment heterogeneous precipitation is likely to be the important mechanism due to the availability of large numbers of potential nucleation sites. Due to the relatively low solubility of calcite (Log K$_{sp}$ = −8.42 ± 0.07; Krauskopf and Bird, 1995), the formation/dissolution of ^{14}C radiolabelled calcite may potentially be an important control on the mobility of ^{14}C-DIC at nuclear sites.

In addition to co-precipitation in carbonates, ^{14}C-DIC can also be removed from solution by isotopic exchange onto calcite surfaces (and other carbonate phases) within the aquifer or soil matrix. Solubility equilibria are dynamic (i.e. dissolution and precipitation rates are equal), so ^{14}C in solution can replace stable C isotopes in mineral carbonates.

$$Ca^{12}CO_{3(s)} + {}^{14}CO_3^{2-}(aq) \rightleftharpoons Ca^{14}CO_{3(s)} + {}^{12}CO_3^{2-}(aq) \qquad (6)$$
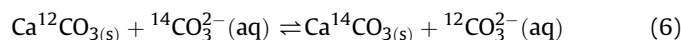
The rate of isotope exchange will depend on the extent of isotope disequilibrium between the solution and carbonate mineral phase, and the dissolution/precipitation kinetics (Sheppard et al., 1997). Pre-existing carbonates will be equilibrated with natural ^{14}C-DIC concentrations, but where ^{14}C is present as a contaminant, ^{14}C-DIC will be present at concentrations far above natural abundance levels, potentially driving rapid exchange kinetics. Indeed, isotope exchange of $H^{14}CO_3^-$ with natural carbonate sand at circumneutral pH was reported to occur on a time scale of only a few days (Garnier, 1985). Isotopic disequilibrium is also the main mechanism in aqueous-gaseous isotopic exchange where disequilibria created by the addition of aqueous ^{14}C species leads to exchange reactions occurring with atmospheric CO_2 to restore isotopic equilibrium among all species of carbonate across the aqueous-gaseous pools (Krauskopf and Bird, 1995; Gonfiantini and Zuppi, 2003; White, 2013). This topic has received extensive academic interest related to the use of both ^{13}C and ^{14}C as tracers of carbon flow between environmental reservoirs, and for ^{14}C for dating carbon-containing material (e.g.; Zhang et al., 1995; Doctor et al., 2008) however, the effect of isotopic equilibrium reactions on ^{14}C behaviour as an environmental contaminant has received far less attention.

The aim of this study was to investigate the factors controlling the mobility of inorganic ^{14}C in near-surface geo-environments. The specific objectives were; (1) to determine the conditions under which inorganic ^{14}C is removed from aqueous solution representative of groundwater by carbonate precipitation reactions; (2) to determine the contribution made by isotopic exchange with calcite in sediments to the loss of inorganic ^{14}C from groundwater; (3) to investigate the rate at which inorganic ^{14}C is lost from solution by isotope exchange with atmospheric CO_2 as a function of aqueous pH, and (4) assess the relative importance of these processes in determining the fate of inorganic ^{14}C in groundwater at the UK Sellafield nuclear site.

2. Materials and methods

2.1. Thermodynamic modelling

Equilibrium geochemical modelling was undertaken using the PHREEQC (version 3) geochemical speciation program (Parkhurst and Appelo, 2013) and the Hatches database (version 18) (Cross and Ewart, 1991) to establish the solution compositions needed to obtain the desired values of SI_{CAL} in the precipitation experiments (see Supporting Information Table S1 for details). Geochemical modelling was also used to investigate the variation of SI_{CAL} with calcium concentration, carbonate alkalinity and pH and to model potential leach scenarios relevant to the UK Sellafield site (section 5).

2.2. Precipitation experiments

A series of Na_2CO_3 solutions were prepared aerobically and equilibrated with atmosphere for a minimum of 72 h by agitation in Erlenmeyer flasks on an orbital shaker (Stuart SSL1; 125 rpm; 16 mm orbit). A series of N_2 purged $CaCl_2$ solutions were also prepared. 10 mL of the required Na_2CO_3 and $CaCl_2$ solutions were mixed in 50 mL Oak Ridge tubes under $N_2(g)$ to produce final solutions (20 mL $\pm$ 0.2 mL) at a range of saturation indices with respect to calcite (SI_{CAL}) from +3 to −1 (see Table 1 for details). 20 μL of ^{14}C-labelled sodium carbonate (pH ~ 12) was added to each tube producing a final activity of 100 Bq mL^{-1} (4.5×10^{-8} M $^{14}CO_3^{2-}$).

Table 1
Solution composition for precipitation experiments. All Na_2CO_3 solutions equilibrated with atmospheric CO_2 for 72 h prior to mixing.

Saturation index	Composition	pH
+3.0	30 mM Na_2CO_3, 20 mM $CaCl_2$	8.97
+2.5	15 mM Na_2CO_3, 15 mM $CaCl_2$	9.07
+2.0	7.5 mM Na_2CO_3, 6 mM $CaCl_2$, 5 mM NaOH	8.89
+1.5	5 mM Na_2CO_3, 15 mM $CaCl_2$, 5 mM NaOH	9.02
+1.0	2.5 mM Na_2CO_3, 0.5 mM $CaCl_2$, 5 mM NaOH	8.88
+0.5	2.5 mM Na_2CO_3, 0.15 mM $CaCl_2$, 5 mM NaOH	8.91
0.0	2.5 mM Na_2CO_3, 0.05 mM $CaCl_2$, 5 mM NaOH	8.93
−1.0	2.5 mM Na_2CO_3, 0.005 mM $CaCl_2$, 5 mM NaOH	9.01

The pH values of the mixtures were adjusted by addition of 5 mM NaOH to maintain the pH value of the Na_2CO_3 solutions used (8.9 $\pm$ 0.1, see Table 1). The mixtures (20 mL $\pm$ 0.2 mL) were sealed in 50 mL Oak Ridge tubes with a $N_2(g)$ filled headspace, and continuously agitated on an end-over-end shaker (Stuart Rotator SB3, 40 rpm). Experiments were prepared in triplicate.

After 168 h, 1.2 mL of sample was removed from each tube and centrifuged for 5 min at 14,000g in 1.5 mL centrifuge tubes. After centrifugation, ^{14}C removal was determined in the supernatant using liquid scintillation counting on a Packard Tri-Carb 2100TR (1 mL sample, 0.1 mL 2 M NaOH, 9 mL PerkinElmer Hionic-Fluor scintillation fluid; count time = 10 min; energy window = 4–156 keV; Caron et al., 2000). Samples were stored for a 24 h period prior to counting. In all tests the percentage of ^{14}C remaining in solution was determined by:

$$\%^{14}C_{aq} = \frac{A_t}{A_i} \times 100 \qquad (7)$$

where A_i is the initial activity at time 0 (counts per minute, CPM), A_t is the activity at a time point (CPM). Solution pH was determined at the beginning and end of experiments using a Thermo Scientific Orion benchtop multimeter, and electrodes calibrated daily at pH 4, 7 and 10. Seeded precipitation experiments similar to the unseeded precipitation experiments described in Table 1 were conducted, where 25 g L^{-1} kaolinite was added to the empty tubes prior to addition of Na_2CO_3 and $CaCl_2$ solutions (K-Ga 1b, Clay Mineral Society, Chantilly, USA). Prior to use in experiments, the kaolinite was acid washed (10% HCl) to remove any carbonate impurities, air-dried and de-aggregated by gentle use of a mortar and pestle. The mineralogical purity of kaolinite was confirmed using X-ray powder diffraction (Cu K-alpha radiation) on a Bruker D8 Advance XRD (see Supporting Information Fig. S1).

2.3. Isotopic exchange experiments

2.3.1. Solid phase isotopic exchange experiments
Equal volumes of 2.5 mM Na_2CO_3 and 0.05 mM $CaCl_2$ solutions were mixed to give a final solution with a pH of 8.87 $\pm$ 0.03 and a calculated $SI_{CAL} = 0$. In triplicate experiments, 50 $\pm$ 0.5 mL aliquots (0.2 μm filtered) of this solution were equilibrated with calcite powder at 0 g L^{-1}, 5 g L^{-1}, 20 g L^{-1} and 50 g L^{-1} (Sigma-Aldrich Reagent Plus) in 50 mL glass serum bottles (Wheaton Scientific Ltd, USA) with N_2 filled headspace, sealed with butyl rubber stoppers (Bellco Glass Inc., USA) and Al crimps. The experimental systems were left for one week to allow calcite dissolution/precipitation equilibration to be established prior to addition of ^{14}C. The bottles were then spiked with 50 μL ^{14}C-labelled sodium carbonate, giving a final activity of 100 Bq mL^{-1}. Periodically 2 mL of solution was removed using sterile, $N_2(g)$ flushed syringes and analysed for ^{14}C activity and pH as described above.

The mineralogical purity of the calcite powder was determined using X-ray powder diffraction (Cu K-alpha radiation) on a Bruker D8 Advance XRD (see Supporting Information Fig. S2). Specific surface area was measured by N_2 gas adsorption using the BET method with a Micrometrics Gemini V Surface Area Analyser (samples degassed with nitrogen gas for a minimum of 19 h, at 60 °C, prior to analysis).

2.3.2. Atmospheric isotopic exchange experiments

Triplicate 100 ± 1 mL experiments were established in 500 mL Erlenmeyer flasks using 0.01 M NaCl as the background electrolyte. The pH was altered using a sodium bicarbonate-carbonate-hydroxide buffer system to give range of experimental pH between pH 7.2 and 12.5 (Table 2). Flasks were equilibrated with atmosphere (in the dark at 20 ± 1 °C) for a minimum of 48 h by shaking at 125 rpm on an orbital shaker prior to $^{14}CO_3^{2-}$ addition. 100 μL of ^{14}C-labelled sodium carbonate was added to each flask, equivalent to 100 Bq mL^{-1}. Periodically 1 mL of solution was removed for ^{14}C analysis, and pH was determined in the flasks. Experiments were continued until either a pH variation of more than ± 0.2 was observed, or less than 5% of initial ^{14}C activity was measured in solution. Parallel triplicate control experiments were established in 30 ml glass serum bottles (sealed with butyl rubber stoppers and Al crimps) where contact with atmosphere was prevented.

3. Results

3.1. Homogeneous and heterogeneous precipitation

In the homogeneous precipitation experiments where the calculated SI_{CAL} was initially between -1.0 and $+1.0$ there was no change in pH over 7 days (in all cases it remained within 0.1 pH units of the initial value 8.9 ± 0.1, see Fig. 1a). In these tests the solutions remained visually clear. In the homogeneous precipitation experiments where SI_{CAL} was initially $+1.5$, $+2.0$, $+2.5$ and $+3.0$, the pH decreased to 8.4, 7.6, 7.2 and 7.6, respectively, over 7 days. A small amount of white precipitate formed in these solutions. ^{14}C tracer removal from these experiments followed a trend with pH change, with no removal observed over a period of 7 days when the initial $SI_{CAL} = -1.0$ to $+1.0$ (Fig. 1b), and progressively more ^{14}C removal with increasing SI_{CAL} values from 1.5 to 3.0 (92–59% of the ^{14}C remained in solution after 7 days).

The heterogeneous precipitation experiments exhibited similar pH trends over time to the homogeneous precipitation experiments (data also shown in Fig. 1). The final pH of all experiments where the initial SI_{CAL} was between -1.0 and $+1.0$ tests was within 0.1 pH units of the starting value, whereas the final pH of all the experiments where the initial SI_{CAL} was $+1.5$ to $+3.0$ was pH 7.5 ± 0.2. However the heterogeneous reactions followed a different trend to the homogeneous reactions with respect to ^{14}C removal (Fig. 1b). Only the $SI_{CAL} = -1.0$ experiment exhibited no ^{14}C removal after 7 days, the $SI_{CAL} = 0$ and 0.5 experiments exhibited a small amount of ^{14}C removal, with progressively more occurring as the

Table 2
Solution composition for atmospheric isotopic exchange experiments.

Solution pH	Composition
7.2	10 mM NaCl, 0.1 mM NaHCO$_3$
8.0	10 mM NaCl, 1 mM NaHCO$_3$
8.8	10 mM NaCl, 10 mM NaHCO$_3$
9.3	10 mM NaCl, 10 mM Na$_2$CO$_3$
10.5	10 mM NaCl, 100 mM Na$_2$CO$_3$, 10 mM NaOH
12.5	10 mM NaCl, 10 mM Na$_2$CO$_3$, 100 mM NaOH

initial SI_{CAL} increased to 3.0 (~20–60% ^{14}C was removed from solution).

3.2. Solid phase isotopic exchange

When calcite was added to saturated calcium carbonate solutions at pH 9.0 the pH remained ± 0.2 pH units for the duration of the experiments (1 month incubation). In the calcite-free (0 g) control experiments no ^{14}C removal occurred over the duration of the experiments (Fig. 2a). In the 5 g L^{-1} calcite ($SA_{BET} = 0.289$ m^2 g^{-1}) experiments there appeared to be a small amount of ^{14}C removal (~2%) after 1 month, but the amount was within the experimental error. For the experiments amended with 20 g L^{-1} calcite there was a removal of 5–6% between 166 and 334 h and a 10% ^{14}C removal at the end of experiments (672 h). The 50 g L^{-1} calcite amended experiments showed a 28% removal at 166 h, the removal at the end of the experiment was 30% of the initial ^{14}C addition (672 h). Overall there was a linear correlation between the total calcite surface area added to each experiment and the observed ^{14}C removal at the end of the experiment (Fig. 2b).

3.3. Atmospheric isotopic exchange

In the closed controls for the experiments investigating ^{14}C exchange with atmosphere, the pH remained constant at the initial values (± 0.2 pH units) from 0 to 264 h (data for up to 100 h is shown in Fig. 3). The ^{14}C activity in these experiments decreased by a small amount over the first 24 h, but ~95% (pH 11 system) or ~93% (pH 9.5 and 7 systems) of the initial activity remained in solution from 24 h to the end of the experiment (264 h). The pH of the open experiments was slightly less stable than that of the closed systems, so these experiments were terminated when the pH change exceeded 0.2 units to ensure comparability of the systems. In the open experiments at pH 12.5, ~100% of the original ^{14}C activity remained in solution at the end of the experiment (48 h). At pH 10.5, 97% of the initial activity remained in solution at the end of the experiment (96 h). At pH 9.3, ^{14}C activity decreased with time (53% remained in solution at 72 h) with only 5% remaining in solution at the end of the experiment (337 h). At pH 8.8, 47% of the initial activity remained in solution at 24 h and only 3% remained in solution at the end of the experiment (121 h). At pH 7.8, 47% of the initial activity remained in solution at 4 h and only 6% remained in solution at the end of the experiment (48 h). At pH 7.0, 48% of the initial activity remained in solution at 1 h and only 1% remained in solution at the end of the experiment (24 h).

4. Discussion

4.1. Effect of seed crystals (nucleation sites) on the precipitation of calcium carbonate

In the calcite precipitation experiments removal of the ^{14}C-DIC tracer indicates that carbonate precipitation occurred in homogeneous systems where the initial $SI_{CAL} \geq 1.5$, and in heterogeneous systems where initial $SI_{CAL} \geq 0-0.5$. These values closely match published SI_{CAL} values for homogeneous and heterogeneous calcite precipitation of 1.5 and 0.3, respectively (White, 1997; Dreybrodt et al., 1992; Ford and Williams, 2007). This close agreement suggests that ^{14}C removal in these experiments was principally controlled by calcite removal. Further it suggests that the solution must be significantly over-saturated with respect to calcite ($SI_{CAL} \geq 1.5$) for it to precipitate in the absence of suitable nucleation sites.

The solution composition required for $SI_{CAL} = 0$ and 1.5 at pH values of 7, 9 and 11 has been modelled using PHREEQC (Fig. 4).
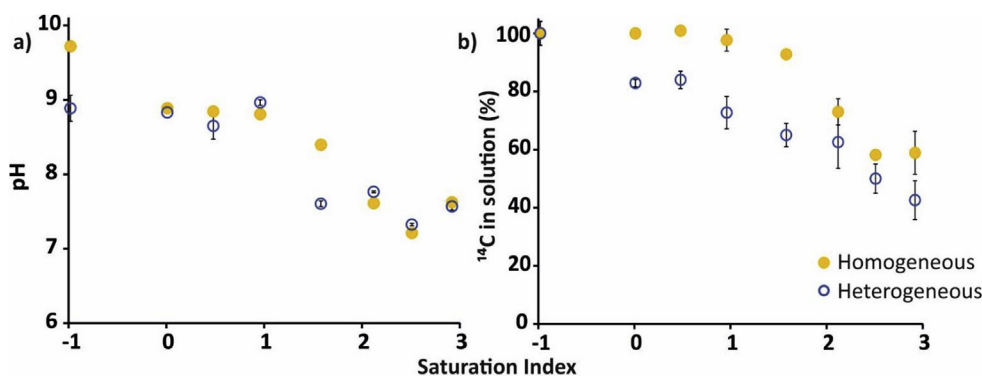
Fig. 1. Homogeneous and heterogeneous precipitation reactions (a) final pH after seven day incubation against the initial predicted saturation index (b) experimental data showing the percentage of ^{14}C in solution after seven day incubation plotted against the predicted initial calcite saturation index of solution (SI$_{CAL}$). Error bars show one standard deviation of triplicate measurements; where not shown, error bars are less than the size of the symbols used.
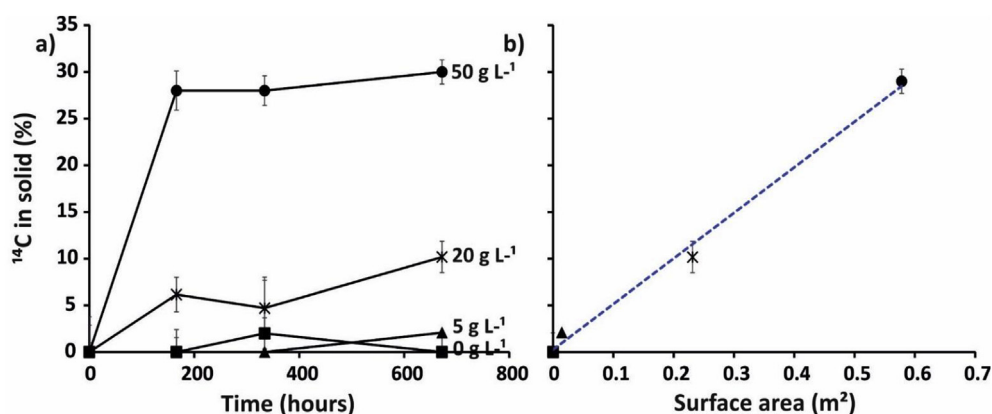

Fig. 2. (a) the amount of ^{14}C associated with the solid phase against time in hours (b) the amount of ^{14}C in solid against the surface area of the calcite after two months incubation. Error bars show one standard deviation of triplicate measurements; where not shown, error bars are less than the size of the symbols used.

These results are sensitive to pH because of the variation in carbonate speciation (reactions 3 and 4), and thus higher concentrations of either Ca^{2+} or carbonate alkalinity are needed to achieve the required (super)saturation indices at lower pH values. In this simulation only heterogeneous precipitation is predicted at circumneutral pH (and even then only at unrealistically high solution concentrations; see Fig. 4a); but at high pH both homogeneous and heterogeneous precipitation reactions are predicted to occur at much lower DIC concentration (Fig. 4b and c) as DIC is mostly speciated as CO_3^{2-} at high pH.

4.2. Contribution of solid phase isotopic exchange to ^{14}C retardation

The solid phase isotope exchange experiments demonstrated that when a solution containing inorganic ^{14}C comes into contact with non-radiolabelled calcite, ^{14}C is removed from solution (Fig. 2) with at least 10% ^{14}C-DIC removal in experiments with $\geq$ 20 g L^{-1} calcite added. The experimental results show that isotopic exchange reached a pseudo-equilibrium after 334 h (approximately two weeks), which was similar to that previously reported by Garnier (1985), where isotopic exchange reached an equilibrium with calcareous soils after one week.

In these experiments, it is available calcite surface area that exhibits a primary control on the observed extent of ^{14}C uptake (Fig. 2b). The kinetics of ^{14}C uptake are governed by the rates of the forward and backward reactions during calcite dissolution/precipitation (see Equation (5)), which at equilibrium are equal leading to

no overall change in calcite mass or DIC concentration. Surface mediated isotopic exchange reactions will therefore proceed rapidly until $^{14/12}$C ratio is equilibrated in the active surface layers of the calcite crystals. It is possible to use the data from the 20 and 50 g L^{-1} experiments to estimate the depth of the active surface layer based on the number of moles of C that must be exchanged to result in an observed 10 and 30% ^{14}C removal (see Supporting Information Section S4 for details). In these calculations, the estimated active surface layer is only 8–10 Å; equating to ~1–2 calcite unit cell thickness (Skinner et al., 1994). This is similar to the theoretical short-term diffusion thickness calculated for ^{45}Ca^{2+} uptake, and the measured thickness for ^{109}Cd uptake by low-energy electron diffraction (Stipp et al., 1992). Stipp et al. (1992) also determined that slow solid state diffusion exchange can occur on much longer timescales (up to 2 years), effectively increasing the active surface layer to several hundred angstroms. Such diffusion driven ^{14}C exchange into carbonate grain interiors could therefore constitute significant additional sinks for ^{14}C-DIC over timescales not observed in these experiments.

Extrapolation of the 20 g L^{-1} calcite experimental conditions to a typical aquifer situation (where the solid solution ratio might be closer to 1:1 w/w) suggests that a 2% w/w calcite concentration in solids is sufficient to reduce the ^{14}C concentration in groundwater by ~10% by rapid exchange with the 10 Å active surface layer, and perhaps more by interparticle diffusion of longer timescales. A 2% calcite concentration is equivalent to a relatively low TIC of 0.24% indicating that isotopic exchange will be an important retardation
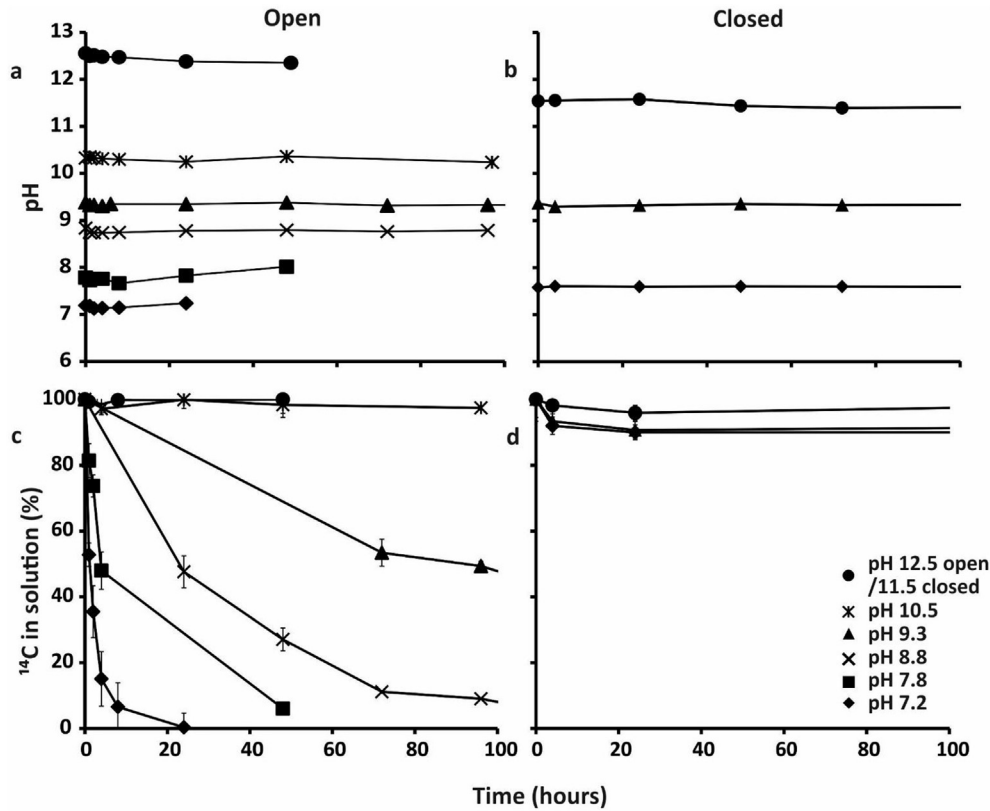
Fig. 3. (a) pH measurement over time in open flask experiments, (b) pH measurement over time in closed bottle experiments, (c) the percentage of ^{14}C remaining in solution over time in open experiments, (d) the percentage of ^{14}C remaining in solution over time in closed experiments. Error bars show one standard deviation of triplicate measurements; where not shown, error bars are less than the size of the symbols used.
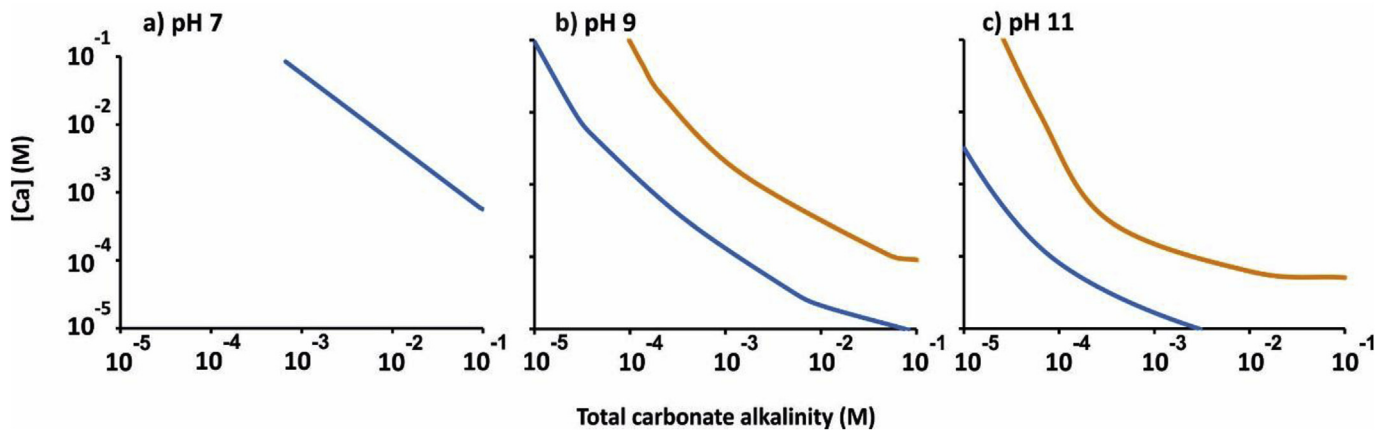

Fig. 4. PHREEQC closed system model predicting the solution compositions necessary for calcite saturation (SI > 0, to the right of the blue line) and homogeneous precipitation (SI > 1.5 to the right of the orange line); (a) at pH 7, (b) at pH 9, and (c) at pH 11. (For interpretation of the references to colour in this figure legend, the reader is referred to the web version of this article.)

process in many near-surface environments with pH values > 6 (n.b. the range of natural soil TIC is 0–12%, although it is completely absent in soils below ~pH 6; Walthert et al., 2010). However, the extent of isotopic exchange will be very sensitive to changes in carbonate surface area, and if carbonates are only present in large detrital grains (with a very low specific surface area), much higher TIC values would be required to cause similar ^{14}C removal (n.b. the surface area of the calcite crystals used in these experiments was 0.29 m² g⁻¹, which is in the typical range 0.17–8.6 m² g⁻¹ used in previous studies of calcite; Nancollas and Reddy, 1971; Inskeep and

Bloom, 1985; Huang et al., 1991; Dreybrodt et al., 1992; but that does not mean it is typical of that found in natural sediments). Also, if TIC is present as less soluble phases (e.g. dolomite; $CaMg(CO_3)_2$; Log Ksp ≈ −18 ± 2; Sherman and Barak, 2000; Stumm and Morgan, 1996), again much slower removal kinetics would be predicted. Therefore, it is very hard to generalise about the specific threshold TIC value where isotopic exchange will become important in the natural environment, and 0.24% w/w is therefore likely to represent a conservative screening threshold. In this context it is interesting to note that the natural aquifer sediments beneath the UK Sellafield

nuclear site have TIC values in the 0—0.6% range (Dutton et al., 2009; Randall et al., 2004) and up to 4.8% in made ground (Randall et al., 2004), and thus, ^{14}C solid isotopic exchange reactions are probably an important retardation mechanism expected to retard ^{14}C-DIC transport in groundwater at this site (especially for locations dominated by made ground).

4.3. Rate of atmospheric isotopic exchange as a function of solution pH

The atmospheric isotopic exchange experiments (Fig. 3) show that there was significant loss of ^{14}C from solutions with pH < 9.3 when there was contact with atmosphere. This loss did not occur in the closed bottle experiments (the 5—7% loss of ^{14}CO$_3^{2-}$ activity from solution observed in the closed experiments was probably associated with CO$_2$ outgassing into the N$_2$-filled headspaces). In all open experiments, pH was stable ($\pm$ 0.2 units) and solutions were well equilibrated with atmospheric CO$_2$ prior to the introduction of ^{14}C as Na$_2$CO$_3$(aq), therefore, there was minimal net outgassing of CO$_2$. It is reasonable to assume that ^{14}C loss is by exchange (at dynamic equilibrium).

Equations 1—4 indicate the steps involved in the exchange of aqueous inorganic carbon species with atmospheric CO$_2$. The equilibrium of these reactions will not have been significantly disturbed by the addition of a small spike of ^{14}CO$_3^{2-}$(aq), but isotopic exchange will have occurred between the inorganic carbon pools because equilibrium is a dynamic state (where the rates of the forward and reverse reaction are equal). If there is a difference in the isotope ratio in the carbon pools driving the forward and reverse reactions, there will be a net transfer of ^{14}C despite the overall reaction being in equilibrium. Protonation/deprotonation reactions such as equations 3 and 4 (acid dissociation constants K$_{a1}$ and K$_{a2}$, respectively) tend to be rapid in aqueous solution (Greenwood and Earnshaw, 1997), and therefore it will be assumed that there is rapid transfer of ^{14}C between the aqueous carbonate pools, and equilibration of their ^{14}C isotope ratios. If the proportion of an aqueous carbonate species, C$_{sp}$ that is ^{14}C$_{sp}$ is x (where x is a function of t) then the following equation can be written for each aqueous carbonate species;

$$\left[^{14}C_{sp}\right] = x\left[C_{sp}\right] \tag{8}$$

At neutral and moderately alkaline pH the outgassing rate of aqueous CO$_2$(aq) (the reverse reaction given by equation 1) is thought to be much faster than its hydration of dissolved CO$_2$ (the forward reaction given by equation 2: Greenwood and Earnshaw, 1997; Appelo and Postma, 2005), so ^{14}C in the dissolved CO$_2$ pool will rapidly equilibrate with the far lower isotope ratio of atmospheric CO$_2$. Thus ^{14}C that is transferred to the aqueous CO$_2$ pool is lost to atmosphere, and the overall rate of ^{14}C loss from the aqueous system is governed by the dehydration of carbonic acid (the reverse of reaction 2). If dehydration is an elementary reaction then the rate equation will have the form:

$$J_{r2} = -d\left[H_2CO_{3(aq)}\right]/dt = k_{r2}\left[H_2CO_{3(aq)}\right] \tag{9}$$

If minor differences in the dehydration rate of different carbon isotopes of carbonic acid are ignored, the overall rate of ^{14}C loss from the aqueous carbonate pools is given by:

$$-d\left[^{14}C_{(aq.carb)}\right]/dt = -d\left[H_2^{14}CO_{3(aq)}\right]/dt = k_{r2}\, x\left[H_2CO_{3(aq)}\right] \tag{10}$$

where x decreases with time, but [H$_2$CO$_{3(aq)}$] is invariant in a

system that is in overall equilibrium with atmospheric CO$_2$. Now:

$$\left[^{14}C_{(aq.carb)}\right] = \left[H_2^{14}CO_{3(aq)}\right] + \left[H^{14}CO_3^-(aq)\right] + \left[^{14}CO_3^{2-}(aq)\right] \tag{11}$$

So at equilibrium:

$$\left[^{14}C_{(aq.carb)}\right] = x\left[H_2CO_{3(aq)}\right] + x\left[HCO_3^-(aq)\right] + x\left[CO_3^{2-}(aq)\right] \tag{12}$$

The acid dissociation constants for equations 3 and 4 are defined as:

$$K_{a1} = \left[H^+_{(aq)}\right]\left[HCO_3^-(aq)\right]/\left[H_2CO_{3(aq)}\right] \text{ and } K_{a2}$$
$$= \left[H^+_{(aq)}\right]\left[CO_3^{2-}(aq)\right]/\left[HCO_3^-(aq)\right]$$

where K$_{a1}$ = 2.5 × 10^{-4} mol L^{-1} and K$_{a2}$ = 4.84 × 10^{-11} mol L^{-1} (Greenwood and Earnshaw, 1997). This K$_{a1}$ value is the true dissociation constant for carbonic acid, whereas many published sources combine reactions 2 and 3 and report the apparent dissociation constant. Equation (12) can be rewritten as:

$$\left[^{14}C_{(aq.carb)}\right] = x\left[H_2CO_{3(aq)}\right]\cdot\left(1 + \frac{K_{a1}}{[H^+]} + \frac{K_{a1}K_{a2}}{[H^+]^2}\right) \tag{13}$$

Which can be substituted in the rate equation (10) to yield

$$\frac{-d\left[^{14}C_{(aq.carb)}\right]}{dt} = \frac{k_{r2}}{\left(1 + \frac{K_{a1}}{[H^+]} + \frac{K_{a1}K_{a2}}{[H^+]^2}\right)}\left[^{14}C_{(aq.carb)}\right] \tag{14}$$

The term $k_{obs} = \dfrac{k_{r2}}{\left(1 + \frac{K_{a1}}{[H^+]} + \frac{K_{a1}K_{a2}}{[H^+]^2}\right)}$ is comparable with the experi-

mental rate constant observed in the atmospheric isotope exchange experiments. Equation (14) can be integrated to yield a rate equation that can be fitted to the experimental data (see Fig. 5):

$$\left[^{14}C_{(aq.carb)}\right] = \left[^{14}C_{(aq.carb)}\right]_o e^{-k_{obs}t} \tag{15}$$

where [^{14}C$_{(aq.carb)}$]$_o$ is the initial concentration of ^{14}C in the aqueous carbonate pool.

Equation (15) has been fitted to all the data from all the atmospheric isotope exchange data by assuming a single value for the dehydration rate for equation (2) of k$_{r2}$ = 4500 hr^{-1} (see Supporting Information S2). Above pH 8 the prediction and experimental data show good agreement. At pH values below 8 the initial rate of ^{14}C loss is greater than predicted by the model, whereas the final ^{14}C concentration are higher than predicted (the latter error is exaggerated on a log scale and not thought significant). The model explicitly assumes dynamic equilibrium between the DIC pools and atmospheric CO$_2$. Addition of an alkaline ^{14}CO$_3^{2-}$-spike to an equilibrated system will have resulted in a brief period of disequilibria, when the out-gassing rate exceeds in-gassing rate. During this period ^{14}C loss is faster than predicted by the model. This effect will have been negligible in higher pH systems due to higher initial CO$_3^{2-}$ concentrations, but may explain the ^{14}C loss in systems with a pH < 8 is faster than predicted by the model.

The linear relationship between the logarithm of ^{14}C concentration and time (Fig. 5b) demonstrates that the loss mechanism is pseudo-first order with respect to ^{14}C concentration. This strongly
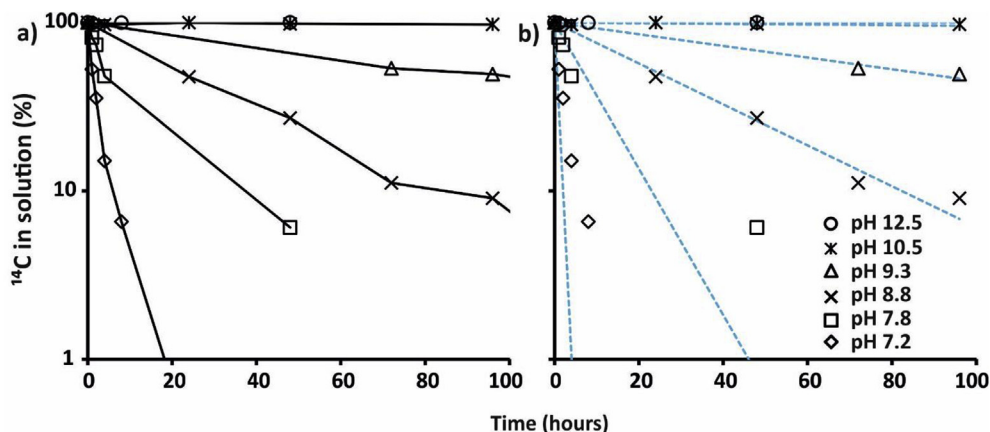
Fig. 5. (a) the experimental results showing the percentage of ^{14}C remaining in solution over time in open system on a log scale (b) experimental data fitted with predicted rate of loss using the derived value of $k_{r2} = 4500$ hr^{-1} for the rate constant.

suggests that the rate of ^{14}C loss is controlled by an elementary reaction that transforms single ^{14}C-bearing molecules. The model assumes that the rate limiting step is dehydration of carbonic acid (equation 2), an assumption that is well supported by the literature (Greenwood and Earnshaw, 1997; Appelo and Postma, 2005). Conversely the overall reaction described in equations 1—4 would also exhibit pseudo-first order kinetics if equation 1 alone (outgassing of dissolved CO_2) was rate limiting (i.e. if reaction 2 was fast in comparison with reaction 1). However it is unlikely that the reaction conditions reported here were so different from other studies that the dehydration step has no influence on the rate, and so the observed pseudo first order kinetics support the assumption that dehydration is rate limiting. Nonetheless the key finding of this study is that any ^{14}C-containing water with a pH < 9.3 that is in contact with atmosphere will rapidly lose $^{14}CO_2$ from solution (timescale of 10's of hours) by isotopic exchange with atmospheric CO_2.

5. Implications

5.1. Implications for surface release of ^{14}C-containing water

Authorised discharge or accidental release of ^{14}C-DIC into surface waters (e.g. at the Sellafield site, UK, ^{14}C-containing effluents are routinely discharged into the Irish Sea; NDA, 2014) would require that the SI$_{CAL}$ values reach +1.5 or greater to initiate ^{14}C removal via homogeneous precipitation reactions. Surface water can contain Ca^{2+}, but often at a lower concentration in comparison to groundwater, thus except in the rare circumstance where very high calcite supersaturation occurs at the point of discharge and mixing, this would facilitate the dilution and dispersal of ^{14}C-DIC in the environment. Precipitation may also be limited by the circumneutral pH of many surface water environments. Authorised discharges are limited to pH range of less than 9, typically falling between pH 5.5 and 9 (Mayes et al., 2009). These conditions would favour atmospheric isotopic exchange which occurs rapidly at pH < 9.3 due to the lower pH of the surface water and discharges. Under these conditions long range transport of ^{14}C-DIC in surface waters is not expected. Indeed, after mixing with surface waters in the Irish Sea, the ^{14}C enriched signal is lost from DIC over a very short spatial zone (Ahad et al., 2006).

5.2. Implication for subsurface release of ^{14}C-containing water

The fate of ^{14}C-DIC released to groundwater will depend on the SI$_{CAL}$ for the combined leak and groundwater. If the mixture remains undersaturated with respect to calcite precipitation, aqueous transport of ^{14}C is very likely to occur, retarded only by isotope exchange with TIC, if present. However, two factors favour the precipitation of calcite in the subsurface. Groundwater often contains Ca^{2+} and Mg^{2+} (and they are important exchangeable cations in most soils), and while the typical pH range of groundwater is similar to that of surface waters, heterogeneous precipitation is favoured by the presence of mineral surfaces. Also, aqueous releases to the subsurface environment are invariably accidental, and therefore the pH value is controlled by the source. If the ^{14}C-DIC source has a high pH value, precipitation is likely to occur over a large range of Ca^{2+} and CO$_3^{2-}$ concentrations (Fig. 4). However, once aqueous release to the subsurface ceases (i.e. the leak is repaired), any precipitate that has formed is likely to dissolve slowly overtime if the local groundwater is undersaturated with respect to calcite (i.e. the neo-formed calcite will become a secondary source term for ^{14}C-DIC).

In organic rich near surface soils, oxidation of organic matter can result in pore air with a partial pressure of $CO_2(g)$ up to 100 times higher than that of atmosphere (Deutsch and Siegel, 1997). The elevated pCO$_2$ value (with respect to atmosphere) indicates that there is poor diffusive CO_2 mass transfer in the vadose zone, possibly because the air and water phases are discontinuous in the vadose zone and the CO_2 must cross numerous phase boundaries. The potential to lose ^{14}C DIC through isotope exchange through the vadose zone, and thence to atmosphere is probably very low (in many situations this isotope exchange must occur against a net TIC flux downwards from the organic rich surface soil). Thus fate of ^{14}C-DIC released to the subsurface is ultimately to be transported by groundwater flow, but this transport may be significantly more retarded than predicted by simple sorption kinetics if the leak source is alkaline or the soil contains significant TIC.

5.3. Historical release of ^{14}C to the subsurface at the UK sellafield site

At the Sellafield reprocessing plant in the UK, there was an accidental discharge of inorganic-^{14}C-containing leachate from the silos containing corroded MAGNOX fuel cladding into the shallow groundwater approximately 40 years ago (Wallace et al., 2012). The corroded magnesium alloy fuel cladding is dominated by brucite with small amounts of hydrous magnesium carbonates and is stored under water (Parry et al., 2011). Ground conditions at the Sellafield site are 1—5 m of made ground above up to 50 m of
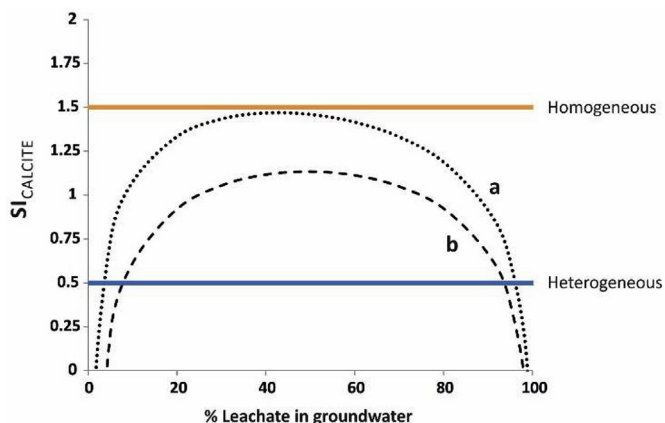
Fig. 6. Predicted saturation indices for the mixing of two potential leachate plumes with groundwater on Sellafield site (a) surface tank composition from the MAGNOX silo (site data − dotted line) (b) deep tank liquor from the MAGNOX silo (modelled − dashed line).

unconsolidated fluvio-glacio till (Stamper et al., 2012; Cruickshank, 2012). The local water table is ~10 m below ground level, therefore, groundwater flow (~200 m a^{-1}) is predominantly within the till and follows the regional hydraulic gradient from east to west across the site (i.e. from the Cumbrian Mountains towards the Irish Sea; Stamper et al., 2012). Groundwater composition varies with location but generally the pH lies between 6 and 8. In the vicinity of the leak the groundwater composition is dominated by Ca-Na-Cl, and the pH is approximately 6.5 (see supporting information S3). Currently the ^{14}C-containing groundwater plume that is associated with the historical leak event is still within the site boundaries and therefore is moving far more slowly than the groundwater.

Two scenarios have been modelled using PHREEQC in order to investigate the potential in situ geochemical conditions during the initial silo leak event. These assume the mixing of either surface or bottom water from within the silos with varying volumes of groundwater. The assumed composition of the water from the surface of the silo is based on site measurements, which showed that it is Na-K-NO$_3$-CO$_3$ dominated with a pH ~9 (Sellafield Ltd, 2009). The silo waters are in contact with atmosphere, so it is assumed for the purposes of modelling the system that this solution was fully equilibrated with atmospheric CO$_2$ (a pH value of 8.8 was used). The silos contain a significant volume of fine material

from the corrosion of magnesium alloy fuel cladding, and therefore the aqueous phase at bottom of the silos may differ significantly from the surface liquor, however, no solution measurements exist for this liquor as it is inaccessible. Therefore this solution has been modelled by assuming it has equilibrated with MgCO$_3$(s) as the most stable magnesium carbonate phase (the final corrosion product of magnesium alloy in an aqueous solution in contact with atmosphere) at a pH of 8.9 (pH at equilibrium with MgCO$_3$, the full solution compositions used in this modelling are given in Supporting Information S3). Modelling with MgCO$_3$(s) gives the most conservative DIC for potential mixture of the deep tank liquor with groundwater. Other hydrous magnesium phases (hydromagnesite; artinite; nesquehonite; and hydrotalcite) have all been predicted/measured within these silo environments (Parry et al., 2011; Gregson et al., 2011), and due to their higher solubility with respect to magnesite, would lead to a higher DIC content in deep tank liquor leading to increased SI$_{CAL}$ over the mixing range.

The PHREEQC modelling indicates that mixing of silo liquor of either composition with the circumneutral groundwater would allow heterogeneous calcite precipitation at almost all mixing ratios (see Fig. 6). Thus it is likely that inorganic ^{14}C in the leak water would be precipitated as calcite. Such calcite precipitation provides a mechanism for retardation of ^{14}C on this site which can explain the long term retention of ^{14}C in the vicinity of the leak sites. At Sellafield the local groundwater has SI$_{CAL}$ < 0 so dissolution of any precipitated calcite and release of ^{14}C to solution is expected over time. The aquifer materials generally contain quite low TIC values of 0−0.6% w/w (except for locations containing made ground) providing limited potential for further additional ^{14}C-DIC retardation by solid isotopic exchange reactions (depending on local ground TIC values close to the silo leaks). As contact with the atmosphere is also limited there is expected to be little loss via atmosphere exchange (although some boreholes may act as conduits facilitating atmospheric isotopic exchange and therefore increase losses of ^{14}C on a local scale). Therefore, over the long-term, ^{14}C stored initially in calcite precipitates is expected to be slowly remobilised and dispersed into groundwater, which ultimately discharges into surface waters (i.e. the Rivers Calder and Ehen or Irish Sea) where it will be rapidly depleted via dilution and exchange with atmospheric ^{12}CO$_2$.

6. Conclusion

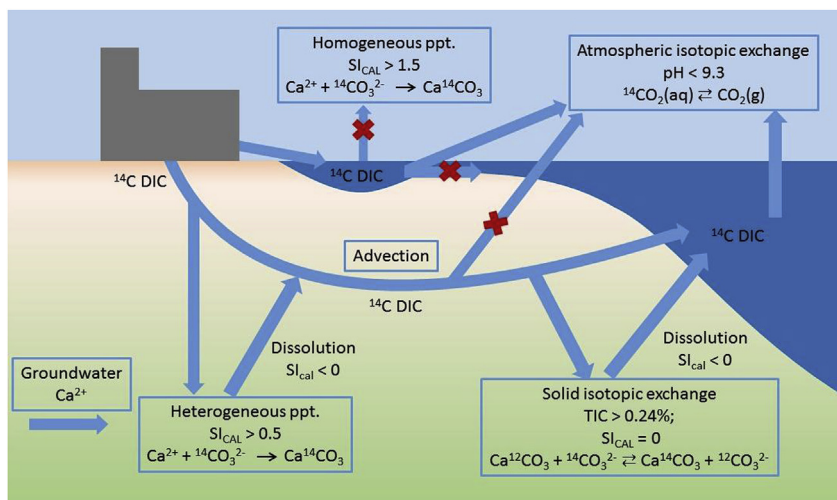Fig. 7 summarises the processes likely to affect ^{14}C-DIC

Fig. 7. Schematic model of processes affecting the ^{14}C-DIC transport in surface and subsurface environments.

behaviour as a surface and near surface contaminant. Many surface waters have a circum-neutral pH and are undersaturated with respect to calcium carbonate. In such environments transfer to atmosphere by isotopic exchange with $^{12}CO_{2\ (g)}$ will be rapid, therefore, if ^{14}C-DIC is discharged into surface water, it is unlikely to be transported very far with the aqueous flow before being lost to atmosphere. In contrast in subsurface conditions, isolation from the atmosphere will prevent loss by exchange with $CO_{2\ (g)}$. Any ^{14}C-DIC release to this environment can potentially be transported with groundwater flow, but carbonate precipitation reactions are likely to be more favoured (by higher pH and Ca^{2+} concentration) and ^{14}C-DIC may be removed from solution and stored within solid carbonate over long timescales. In moderately calcareous environments (with TIC > ~0.24% w/w) isotopic exchange of the ^{14}C-DIC with ^{12}C-containing carbonates is also expected to retain ^{14}C in the solid fraction. Thus, retarded ^{14}C-DIC transport can be expected in the near field environment at many nuclear sites and ^{14}C contamination may persist in sub-surface environments for decades following any accidental releases to ground.

Acknowledgements

Appendix A. Supplementary data

Supplementary data related to this article can be found at http://dx.doi.org/10.1016/j.apgeochem.2016.12.006.

References

Ahad, J.M., Ganeshram, R.S., Spencer, R.G., Uher, G., Gulliver, P., Bryant, C.L., 2006. Evidence for anthropogenic 14C-enrichment in estuarine waters adjacent to the North Sea. Geophys. Res. Lett. 33 (8).

Appelo, C.A.J., Postma, D., 2005. Geochemistry, Groundwater and Pollution, second ed. Taylor & Francis.

Atkins, P.W., De Paula, J., 2006. Atkins' Physical Chemistry. Macmillan Higher Education.

Baston, G.M.N., Marshall, T.A., Otlet, R.L., Walker, A.J., Mather, I.D., Williams, S.J., 2012. Rate and speciation of volatile carbon-14 and tritium releases from irradiated graphite. Mineral. Mag. 76, 3293–3302.

Begg, F.H., Cook, G.T., Baxter, M.S., Scott, E.M., McCartney, M., 1992. Anthropogenic radiocarbon in the eastern Irish Sea and Scottish coastal waters. Radiocarbon 34, 707–716.

Bird, G.A., Bergström, U., Nordlinder, S., Neal, S.L., Smith, G.M., 1999. Model simulations of the fate of 14C added to a Canadian shield lake. J. Environ. Radioact. 42, 209–223.

Bischoff, W.D., Bishop, F.C., Mackenzie, F.T., 1983. Biogenically produced magnesian calcite: inhomogeneities in chemical and physical properties: comparison with synthetic phases. Am. Mineralogist 68, 1183–1188.

Boss, C., Allsop, P.J., 1995. Radioactive Effluents from CANDU 6 Reactors during Normal Operation. Atomic Energy of Canada Ltd.

Bracke, G., Müller, W., 2008. Contribution to a more realistic approach in assessing the release of C-14 from low-level radioactive waste repositories. J. Contam. Hydrology 102 (3), 210–216.

Caron, F., Sutton, J., Benz, M.L., Haas, M.K., 2000. Determination of carbon-14 levels in heavy water and groundwaters. Analyst 125, 59–64.

Cook, G.T., MacKenzie, A.B., Naysmith, P., Anderson, R., 1998. Natural and anthropogenic 14C in the UK coastal marine environment. J. Environ. Radioact. 40, 89–111.

Cross, J.E., Ewart, F.T., 1991. Hatches — a thermodynamic database and management system. Radiochim. Acta 52–53, 421–422.

Cruickshank, J., 2012. Findings of the Sellafield Contaminated Land and Groundwater Management [Online]. Sellafield Ltd. Available. http://www.sellafieldsites.com/land/documents/Signpost%20Report.pdf [Accessed 19/03 2014].

Deutsch, W.J., Siegel, R., 1997. Groundwater geochemistry: fundamentals and applications to contamination. Taylor & Francis.

Doctor, D.H., Kendall, C., Sebestyen, S.D., Shanley, J.B., Ote, N., Boyer, E.W., 2008.

Carbon isotope fractionation of dissolved inorganic carbon (DIC) due to outgassing of carbon dioxide from a headwater stream. Hydrol. Process. 22, 2410–2423.

Doulgeris, C., Humphreys, P., Rout, S., 2015. An approach to modelling the impact of 14C release from reactor graphite in a geological disposal facility. Mineral. Mag. 79, 1495–1503.

Dreybrodt, W., Buhmann, D., Michaelis, J., Usdowski, E., 1992. Geochemically controlled calcite precipitation by CO2 outgassing: field measurements of precipitation rates in comparison to theoretical predictions. Chem. Geol. 97, 285–294.

Dutton, M.V., Foster, C., Trivedi, D., 2009. Characterisation of Soils from Site Investigation within the Sellafield Separation Area. NNL Commercial.

Eabry, S., Vance, J.N., Cline, J.E., Robertson, D.E., 1995. Characterization of Carbon-14 Generated by the Nuclear Power Industry: Final Report. Electric Power Research Institute.

Evenden, W.G., Sheppard, S.C., Killey, R.W.D., 1998. Carbon-14 and tritium in plants of a wetland containing contaminated groundwater. Appl. Geochem. 13, 17–21.

Ford, D., Williams, P.D., 2007. Karst Hydrogeology and Geomorphology. Wiley.

Garnier, J.M., 1985. Retardation of dissolved radiocarbon through a carbonated matrix. Geochimica Cosmochimica Acta 49, 683–693.

Godwin, H., 1962. Half-life of radiocarbon. Nature 195, 984.

Gonfiantini, R., Zuppi, G.M., 2003. Carbon isotope exchange rate of DIC in karst groundwater. Chem. Geol. 197, 319–336.

Greenwood, N.N., Earnshaw, A., 1997. Chemistry of the Elements, second ed. Pergamon Press.

Gregson, C.R., Goddard, D.T., Sarsfield, M.J., Taylor, R.J., 2011. Combined electron microscopy and vibrational spectroscopy study of corroded Magnox sludge from a legacy spent nuclear fuel storage pond. J. Nucl. Mater. 412 (1), 145–156.

Gu, B., Schulz, R.K., 1991. Anion Retention in Soil: Possible Application to Reduce Migration of Buried Technetium and Iodine. Nuclear Regulatory Commission, Washington, DC (United States). Div. Of Regulatory Applications (Dept. of Soil Science). California Univ., Berkeley, CA (United States).

Hodkin, D.J., Stewart, D.I., Graham, J.T., Burke, I.T., 2016. Coprecipitation of 14C and Sr with carbonate precipitates: the importance of reaction kinetics and recrystallization pathways. Sci. Total Environ. 562, 335–343.

Huang, Y.C., Fowkes, F.M., Lloyd, T.B., Sanders, N.D., 1991. Adsorption of calcium ions from calcium chloride solutions onto calcium carbonate particles. Langmuir 7, 1742–1748.

Inskeep, W.P., Bloom, P.R., 1985. An evaluation of rate equations for calcite precipitation kinetics at pCO2 less than 0.01 atm and pH greater than 8. Geochimica Cosmochimica Acta. 49, 2165–2180.

Jackson, C.P., Yates, H., 2011. Key Processes and Data for the Migration of 14C Released from a Cementitious Repository, Serco Report.

Killey, R.W.D., Rao, R.R., Eyvindson, S., 1998. Radiocarbon speciation and distribution in an aquifer plume and groundwater discharge area, Chalk River, Ontario. Appl. Geochem. 13, 3–16.

Krauskopf, K.B., Bird, D.K., 1995. Introduction to Geochemistry. McGraw-Hill.

Langmuir, D., 1997. Use of laboratory adsorption data and models to predict radionuclide releases from a geological repository: A brief history, Materials Research Society Symposium - Proceedings, pp. [d]769–780.

Limer, L.M.C., Thorne, M.C., Cummings, R., 2011. Consideration of canopy structure in modelling 14C-labelled gas behaviour in the biosphere for human dose assessments. Radioprotection 46, S409–S415.

Limer, L, Klos, R., Walke, R., Shaw, G., Norden, M., Xu, S., 2013. Soil-plant-atmosphere modelling in the context of releases of 14C as a consequence of nuclear activities. Radiocarbon 55, 804–813.

Sellafield Ltd, 2009. Generic Basis for Inventory Challenge — Legacy Alkaline Sludge Systems. Sellafield Ltd., Cumbria, UK.

Magnusson, A., Stenstrom, K., Skog, G., Adliene, D., Adlys, G., Hellborg, R., Olariu, A., Zakaria, M., Raaf, C., Mattsson, S., 2004. Levels of ^{14}C in the terrestrial environment in the vicinity of two european nuclear power plants. Radiocarbon 46 (2), 863–868.

Marshall, T.A., Baston, G.M.N., Otlett, R.L., Walker, A.J., Mather, I.D., 2011. Longer-term Release of Carbon-14 from Irradiated Graphite [Online]. Available. http://www.nda.gov.uk/publication/longer-term-release-of-carbon-14-from-irradiated-graphite-october-2011/ [Accessed 31/10/2013].

Marshall, A., Coughlin, D., Laws, F., 2015. Groundwater Monitoring at Sellafield: Annual Data Review 2014.

Mayes, W.M., Johnston, D., Potter, H.A.B., Jarvis, A.P., 2009. A national strategy for identification, prioritisation and management of pollution from abandoned non-coal mine sites in England and Wales. I. Methodology development and initial results. Sci. Total Environ. 407, 5435–5447.

Mucci, A., Morse, J.W., 1983. The incorporation of Mg2+ and Sr2+ into calcite overgrowths: influences of growth rate and solution composition. Geochimica Cosmochimica Acta. 47, 217–233.

Nancollas, G.H., Reddy, M.M., 1971. The crystallization of calcium carbonate. II. Calcite growth mechanism. J. Colloid Interface Sci. 37 (4), 824–830.

NDA, 2012. Geological Disposal: Carbon-14 Project - Phase 1 Report. Nuclear Decommissioning Authority.

NDA, 2014. Monitoring Our Environment: Discharges and Environmental Monitoring. Nuclear Decommissioning Authority.

Parkhurst, D.L., Appelo, C.A.J., 2013. Description of input and examples for PHREEQC version 3- A computer program for speciation, batch-reaction, one-dimensional transport, and inverse geochemical calculations, U.S. Geol. Surv. Tech. Methods. 497.

Parry, S.A., O'Brien, L., Fellerman, A.S., Eaves, C.J., Milestone, N.B., Bryan, N.D., Livens, F.R., 2011. Plutonium behaviour in nuclear fuel storage pond effluents. Energy & Environ. Sci. 4, 1457—1464.

Plummer, L.N., Busenberg, E., 1982. The solubilities of calcite, aragonite and vaterite in CO2-H2O solutions between 0 and 90°C, and an evaluation of the aqueous model for the system CaCO3-CO2-H2O. Geochimica Cosmochimica Acta. 46, 1011—1040.

Randall, M.G., Brydie, J., Graham, J., Small, J.S., 2004. SCLS Phase 1: the Geochemistry of the Sellafield Site. BNFL Commercial.

Roussel-Debet, S., Gontier, G., Siclet, F., Fournier, M., 2006. Distribution of carbon 14 in the terrestrial environment close to French nuclear power plants. J. Environ. Radioact. 87 (3), 246—259.

Sheppard, M.I., Elrick, D.E., Peterson, S.R., 1997. Review and performance of four models to assess the fate of radionuclides and heavy metals in surface soil. Can. J. Soil Sci. 77, 333—344.

Sheppard, S.C., Ticknor, K.V., Evenden, W.G., 1998. Sorption of inorganic 14C on to calcite, montmorillonite and soil. Appl. Geochem. 13, 43—47.

Sherman, L.A., Barak, P., 2000. Solubility and dissolution kinetics of dolomite in Ca—Mg—HCO3/CO3 solutions at 25°C and 0.1 MPa carbon dioxide. Soil Sci. Soc. Am. J. 64, 1959—1968.

Skinner, A.J., LaFemina, J.P., Jansen, H.J.F., 1994. Structure and bonding of calcite; a theoretical study. Am. Mineralogist. 79 (3—4), 205—214.

Stamper, A., McKinlay, C., Coughlin, D., Laws, F., 2012. Land Quality Programme Groundwater Monitoring at Sellafield [Online]. Sellafield Ltd. Available. http://www.sellafieldsites.com/land/documents/Groundwater%20Monitoring%20at%20Sellafield%20-%20Annual%20Data%20Review%202012.pdf [Accessed 19/03 2014].

Stipp, S.L., Hochella, M.F., Parks, G.A., Leckie, J.O., 1992. Cd2+ uptake by calcite, solid-state diffusion, and the formation of solid-solution: interface processes observed with near-surface sensitive techniques (XPS, LEED, and AES). Geochimica Cosmochimica Acta. 56 (5), 1941—1954.

Stumm, W., Morgan, J.J., 1996. Aquatic Chemistry: Chemical Equilibria and Rates in Natural Waters. Wiley.

Su, C., Suarez, D.L., 1997. In situ infrared speciation of adsorbed carbonate on aluminum and iron oxides. Clays Clay Minerals. 45, 814—825.

van Geen, A., Robertson, A.P., Leckie, J.O., 1994. Complexation of carbonate species at the goethite surface: implications for adsorption of metal ions in natural waters. Geochimica Cosmochimica Acta. 58, 2073—2086.

Wallace, S.H., Shaw, S., Morris, K., Small, J.S., Fuller, A.J., Burke, I.T., 2012. Effect of groundwater pH and ionic strength on strontium sorption in aquifer sediments: implications for 90Sr mobility at contaminated nuclear sites. Appl. Geochem. 27, 1482—1491.

Walthert, L., Graf, U., Kammer, A., Luster, J., Pezzotta, D., Zimmerman, S., Hagedorn, F., 2010. Determination of organic and inorganic carbon, δ13C, and nitrogen in soils containing carbonates after acid fumigation with HCl. J. Plant Nutr. Soil Sci. 173, 207—216.

White, W., 1997. Thermodynamic equilibrium, kinetics, activation barriers, and reaction mechanisms for chemical reactions in karst terrains. Environ. Geol. 30, 46—58.

White, W., 2013. Geochemistry. Wiley-Blackwell.

Wijnja, H., Schulthess, C.P., 2000. Interaction of carbonate and organic anions with sulfate and selenate adsorption on an aluminum oxide. Soil Sci. Soc. Am. J. 64, 898—908.

Yim, M.-S., Caron, F., 2006. Life cycle and management of carbon-14 from nuclear power generation. Prog. Nucl. Energy. 48, 2—36.

Zhang, J., Quay, P.D., Wilbur, D.O., 1995. Carbon isotope fractionation during gas-water exchange and dissolution of CO2. Geochimica Cosmochimica Acta. 59, 107—114.